1.11

QUASIPARTICLE AND OPTICAL PROPERTIES OF SOLIDS AND NANOSTRUCTURES: THE GW-BSE APPROACH

Steven G. Louie[1] and Angel Rubio[2]
[1]*Department of Physics, University of California at Berkeley and Materials Sciences Division, Lawrence Berkeley National Laboratory, Berkeley, CA 94720, USA*
[2]*Departamento Física de Materiales and Unidad de Física de Materiales Centro Mixto CSIC-UPV, Universidad del País Vasco and Donosita Internacional Phycis Center (DIPC)*

We present a review of recent progress in the first-principles study of the spectroscopic properties of solids and nanostructures employing a many-body Green's function approach based on the GW approximation to the electron self-energy. The approach has been widely used to investigate the excited-state properties of condensed matter as probed by photoemission, tunneling, optical, and related techniques. In this article, we first give a brief overview of the theoretical foundations of the approach, then present a sample of applications to systems ranging from extended solids to surfaces to nanostructures and discuss some possible ideas for further developments.

1. Background

A large part of research in condensed matter science is related to the characterization of the electronic properties of interacting many-electron systems. In particular, an accurate description of the electronic structure and its response to external probes is essential for understanding the behavior of systems ranging from atoms, molecules, and nanostructures to complex materials. Moreover, many characterization tools in physics, chemistry and materials science as well as electro/optical devices are spectroscopic in nature, based on the interaction

S. Yip (ed.),
Handbook of Materials Modeling, 215–240.

of photons, electrons, or other quanta with matter exciting the system to higher energy states. Yet, many fundamental questions concerning the conceptual and quantitative descriptions of excited states of condensed matter and their interactions with external probes are still open. Hence there is a strong need for theoretical approaches which can provide an accurate description of the excited-state electronic structure of a system and its response to external probes. In what follows we discuss some recent progress along a very fruitful direction in the first-principles studies of the electronic excited-state properties of materials, employing a many-electron Green's function approach based on the so-called GW approximation [1–3].

Solving for the electronic structure of an interacting electron system (in terms of the many-particle Schrödinger equation) has an intrinsic high complexity: while the problem is completely well defined in terms of the total number of particles N and the external potential $V(\mathbf{r})$, its solution depends on $3N$ coordinates. This makes the direct search for either exact or approximate solutions to the many-body problem a task of rapidly increasing complexity. Fortunately, in the study of either ground- or excited-state properties, we seldom need the full solution to the Schrödinger equation. When one is interested in structural properties, the ground-state total energy is sufficient. In other cases, we want to study how the system responds to some external probe. Then knowledge of a few excited-state properties must be added. For instance, in a direct photoemission experiment, a photon impinges on the system and an electron is removed. In an inverse photoemission process, an electron is absorbed and a photon is ejected. In both cases we just have to deal with the gain or loss of energy of the N electron system when a single particle is added or removed, i.e., with the one-particle excitation spectrum. If the electron was not removed after the absorption of the photon, the system evolves from its ground state to a neutral excited state, and the process may be described by correlated electron–hole excitation amplitudes.

At the simplest level of treating the many-electron problem, the Hartree–Fock theory (HF) is obtained by considering the ground-state wavefunction to be a single Slater determinant of single-particle orbitals. In this way the N-body problem is reduced to N one-body problems with a self-consistent requirement due to the dependence of the HF effective potential on the wavefunction. By the variational theorem, the HF total energy is a variational upper bound of the ground-state energy for a particular symmetry. The HF-eigenvalues may also be used as rough estimates of the one-electron excitation energies. The validity of this procedure hinges on the assumption that the single-particle orbitals in the N and (N-1) system are the same (Koopman's theorem), i.e., neglecting the electronic relaxation of the system. A better procedure to estimate excitation energies is to perform self-consistent calculations for the N and (N-1) systems and subtract the total energies (this is called the "Δ-SCF method" for excitation energies which has also been used in other theoretical frameworks such as the

density-functional theory). For infinitely extended system, this scheme gives the same result as Koopman's theorem and more refined methods are needed to address the problem of one-particle (quasiparticle) excitation energies in solids. The HF theory in general is far from accurate because typically the wavefunction of a system cannot be written as a single determinant for the ground state and Koopman's theorem is a poor approximation.

On the other hand, within density-functional-theory (DFT), the ground-state energy of an interacting system can be exactly written as a functional of the ground-state electronic density [4]. When comparing to conventional quantum chemistry methods, this approach is particularly appealing since solving the ground-state energy does not rely on the complete knowledge of the N-electron wavefunction but only on the electronic density, reducing the problem to that of a self-consistent field calculation. However, although the theory is exact, the energy functional contains an unknown quantity called the exchange-correlation energy, $E_{\mathrm{xc}}[n]$, that has to be approximated in practical implementations. For ground-state properties, in particular those of solids and larger molecular systems, present-day DFT results are comparable or even surpassing in quality to those from standard *ab initio* quantum chemistry techniques. Its use has continued to increase due to a better scaling in computational effort with the number of atoms in the system.

As in HF theory, the Kohn–Sham eigenvalues of the DFT cannot be directly interpreted as the quasiparticle excitation energies. Such interpretation has led to the well-known bandgap problem for semiconductors and insulators: the Kohn–Sham gap is typically 30–50% less than the observed band gap. Indeed, the original formulation of the DFT is not applicable to excited states nor to problems involving time-dependent external fields, thus excluding the calculation of optical response, quasiparticle excitation spectrum, photochemistry, etc. Theorems have, however, been proved subsequently for time-dependent density functional theory (TDDFT) which extends the applicability of the approach to excited-state phenomena [5, 6]. The main result of TDDFT is a set of time-dependent Kohn–Sham equations that include all the many-body effects through a time-dependent exchange-correlation potential. As for static DFT, this potential is unknown and has to be approximated in any practical application. TDDFT has been applied with success to the calculations of quantities such as the electron polarizabilities for the optical spectra of finite systems. However, TDDFT encounters problems in studying spectroscopic properties of extended systems [7] and severely underestimates the high-lying excitation energies in molecules when simple exchange and correlation functionals are employed. These failures are related to our ignorance of the exact exchange-correlation potential in DFT. The actual functional relation between density, $n(\mathbf{r})$, and the exchange-correlation potential, $V_{\mathrm{xc}}(\mathbf{r})$, is highly non-analytical and non-local. A very active field of current research is in the search of robust, new exchange-correlation functionals for real material applications.

Alternatively, a theoretically well-grounded and rigorous approach for the excited-state properties of condensed matter is the interacting Green's function approach. The n-particle Green's function describes the propagation of the n-particle amplitude in an interacting electron system. It provides a proper framework for accurately computing the N-particle excitation properties. For example, knowledge of the one-particle and two-particle Green's functions yields information, respectively, on the quasiparticle excitations and optical response of a system. The use of this approach for practical study of the spectroscopic properties of real materials is the focus of the present review.

In the remainder of the article, we first present a brief overview of the theoretical framework for many-body perturbation theory and discuss the first-principles calculation of properties related to the one- and two-particle Green's functions within the GW approximation to the electron self-energy operator. Then, we present some selected examples of applications to solids and reduced dimensional systems. Finally, some conclusions and perspectives are given.

2. Many-body Perturbation Theory and Green's Functions

A very successful and fruitful development for computing electron excitations has been a first-principles self-energy approach [1–3, 8] in which the quasiparticle's (excited electron or hole) energy is determined directly by calculating the contribution of the dynamical polarization of the surrounding electrons. In many-body theory, this is obtained by evaluating the evolution of the amplitude of the added particle via the single-particle Green's function, $G(xt, x't') = -i\langle N|T\{\psi(xt)\psi^\dagger(x't')\}|N\rangle$,* from which one obtains the dispersion relation and lifetime of the quasiparticle excited state. There are no adjustable parameters in the theory and, from the equation of motion of the single-particle Green's function, the quasiparticle energies $E_{\rm nk}$ and wavefunctions $\psi_{\rm nk}$ are determined by solving a Schrödinger-like equation:

$$(T + V_{\rm ext} + V_{\rm H})\psi_k(\mathbf{r}) + \int d\mathbf{r}\,\Sigma(\mathbf{r},\mathbf{r}';E_{\rm nk})\psi_{\rm nk}(\mathbf{r}') = E_{\rm nk}\psi_{\rm nk}(\mathbf{r}), \qquad (1)$$

where T is the kinetic energy operator, $V_{\rm ext}$ is the external potential due to the ions, $V_{\rm H}$ is the Hartree potential of the electrons, and Σ is the self-energy operator where all the many-body exchange and correlation effects are included. The self-energy operator describes an effective potential on the quasiparticle

*This corresponds to the Green's function at zero temperature where $|N>$ is the many-electron ground state, $\psi(xt)$ is the field operator in the Heisenberg picture, x stands for the spatial coordinates $\mathbf{r}$ plus the spin coordinate, and T is the time ordered operator. In this context, $\psi^\dagger(xt)|N>$ represents an $(N+1)$-electron state in which an electron has been added at time t onto position $\mathbf{r}$.

resulting from the interaction with all the other electrons in the system. In general Σ is non-local, energy dependent and non-Hermitian, with the imaginary part giving the lifetime of the excited state. Similarly, from the two-particle Green's function, we can obtain the correlated electron–hole amplitude and excitation spectrum, and hence the optical properties.

For details of the Green's function formalism and many-body techniques applied to condensed matter, we refer the reader to several comprehensive papers in the literature [2, 3, 7–10]. Here we shall just present some of the main equations used for the quasiparticle and optical spectra calculations. (To simplify the presentation, we use in the following atomic units, $e = \hbar = m = 1$.) In standard textbook, the unperturbed system is often taken to be the non-interacting system of electrons under the potential $V_{\text{ion}}(\mathbf{r}) + V_{\text{H}}(\mathbf{r})$. However, for rapid convergence in a perturbation series, it is better to start from a different non-interacting or mean-field scenario, like the Kohn–Sham DFT system, which already includes an attempt to describe exchange and correlations in the actual system. Also, in a many-electron system, the Coulomb interaction between two electrons is readily screened by a dynamic rearrangement of the other electrons, reducing its strength. It is more natural to describe the electron–electron interaction in terms of a screened Coulomb potential W and formulate the self energy as a perturbation series in terms of W. In this approach [1–3], the electron self-energy can then be obtained from a self-consistent set of Dyson-like equations:

$$P(12) = -i \int \mathrm{d}(34) G(13) G(41^+)\, \Gamma(34, 2) \tag{2}$$

$$W(12) = v(12) + \int \mathrm{d}(34) W(13) P(34) v(42) \tag{3}$$

$$\Sigma(12) = i \int \mathrm{d}(34) G(14^+) W(13) \Gamma(42, 3) \tag{4}$$

$$G(12) = G_0(12) + \int \mathrm{d}(34) G_0(13) [\Sigma(34) - \delta(34) V_{\text{xc}}(4)] G(42) \tag{5}$$

$$\Gamma(12, 3) = \delta(12)\delta(13) + \int \mathrm{d}(4567) [\delta\Sigma(12)/\delta G(45)] \times G(46) G(75) \Gamma(67, 3) \tag{6}$$

where $1 \equiv (x_1, t_1)$ and $1^+ \equiv (x_1, t_1 + \eta)(\eta > 0$ infinitesimal). v stands for the bare Coulomb interaction, P is the irreducible polarization, W is the dynamical screened Coulomb interaction, and Γ is the so-called vertex function. Here G_0 is the single-particle DFT Green's function, $G_0(x, x'; \omega) = \sum_n \psi_n(x) \psi_n^*(x)/[\omega - \varepsilon_n - i\eta \mathrm{sgn}(\mu_n)]$, with η a positive infinitesimal and ψ_n and ε_n the corresponding DFT wavefunctions and eigenenergies. This way of writing down the equations is in fact appealing since it highlights the important physical ingredients: the polarization (which contains the response of the system to the additional particle or hole) is built up by the creation of particle–hole pairs

(described by the two-particle Green's functions). The vertex function Γ contains the information that the hole and the electron interact. This set of equations defines an iterative approach that allows us to gather information about quasiparticle excitations and dynamics. The iterative approach of course has to be approximated. We now describe some of the approximations used in the literature to address quasiparticle excitations and their subsequent extension to optical spectroscopy and exciton states.

3. Quasiparticle Excitations: the GW Approach

In practical first-principles implementations, the GW approximation [1] is employed in which the self-energy operator Σ is taken to be the first order term in a series expansion in terms of the screened Coulomb interaction W and the dressed Green function G of the electron

$$P(12) = -iG(12)G(21) \tag{7}$$

$$\Sigma(12) = iG(12^+)W(12) \tag{8}$$

(in frequency space: $\Sigma(\mathbf{r}, \mathbf{r}'; \omega) = i/2\pi \int d\omega' \mathrm{e}^{-i\omega'\eta} G(\mathbf{r}, \mathbf{r}', \omega - \omega') W(\mathbf{r}, \mathbf{r}', \omega')$). Vertex corrections are not included in this approximation. This corresponds to the simplest approximation for $\Gamma(123)$, assuming it to be diagonal in space and time coordinates, i.e., $\Gamma(123) = \delta(12)\delta(13)$. This has to be complemented with Eq. (5) above. Thus, even at the GW level, we have a many-body self-consistent problem. Most *ab initio* GW applications do this self-consistent loop by (1) taking the DFT results as the mean field and (2) varying the energy of the quasiparticle but keeping fixed its wavefunction (equal to the DFT wavefunction). This corresponds to the G_0W_0 scheme for the calculation of quasiparticle energy as a first-order perturbation to the Kohn–Sham energy ε_{nk}:

$$E_{\mathrm{nk}} \approx \varepsilon_{\mathrm{nk}} + \langle nk|\Sigma(E_{\mathrm{nk}}) - V_{\mathrm{xc}}|nk\rangle, \tag{9}$$

where V_{xc} is the exchange-correlation potential within DFT and $|nk>$ is the corresponding wavefunction. This "G_0W_0" approximation reproduces to within 0.1 eV the experimental band gaps for many semiconductors and insulators and their surfaces, thus circumventing the well-known bandgap problem [2, 3]. Also it gives much better HOMO–LUMO gaps and ionization energies in localized systems, and results for the lifetimes of hot electrons in metals and image states at surfaces [7]. For some systems, the quasiparticle wavefunction can differ significantly from the DFT wavefunction; one then needs to solve the quasiparticle equation, Eq. (1), directly.

4. Optical Response: the Bethe–Salpeter Equation

From Eqs. (2)–(6) for the GW self energy, we have a non-vanishing functional derivative $\delta\Sigma/\delta G$. One obtains a second-order correction to the bare vertex $\Gamma^{(1)}(123) = \delta(12)\delta(13)$:

$$\Gamma^{(2)}(123) = \delta(12)\delta(13) + \int \mathrm{d}(4567)[\delta\Sigma^{(1)}(12)/\delta G_0(45)]G_0(46) \times G_0(75)\Gamma^{(1)}(673). \tag{10}$$

This can be viewed as the linear response of the self-energy to a change in the total potential of the system. The vertex correction accounts for exchange-correlation effects between an electron and the other electrons in the screening density cloud. In particular it includes the electron–hole interaction (excitonic effects) in the dielectric response*. Indeed, the functional derivative of G is responsible for the attractive direct term in the electron–hole interaction that goes into the effective two-particle equation, the Bethe–Salpeter equation, which determines the spectrum and wavefunctions of the correlated electron–hole neutral excitations created, for example, in optical experiments. Taking as first-order self energy $\Sigma^{(1)} = G_0 W_0$, it is easy to derive a Bethe–Salpeter equation, which correctly yields features like bound excitons and changes in absorption strength in the optical absorption spectra. Within this scheme [7, 10], the effective two-particle Hamiltonian takes (when static screening is used in W) a particularly simple, energy-independent form

$$\sum_{n3n4}[(\varepsilon_{n1} - \varepsilon_{n2})\delta_{n1n3}\delta_{n2n4} + u_{(n1n2)(n3n4)} - W_{(n1n2)(n3n4)}]A_{\mathrm{S}}^{(n3n4)} = \Omega_{\mathrm{S}}\mathrm{A_S}^{(n1n2)} \tag{11}$$

where A_{S} is the electron–hole amplitude and the matrix elements are taken with respect to the quasiparticle wavefunctions $n_1, \ldots, n_4$ as follows: $u_{(n1n2)(n3n4)} = \langle n_1 n_2|u|n_3 n_4\rangle$ and $W_{(n1n2)(n3n4)} = \langle n_1 n_3|W|n_2 n_4\rangle$, with u equal to the Coulomb potential v except for the long-range component $q = 0$ that is set to zero (that is, $u(q) = 4\pi/q^2$ but with $u(0) = 0$). The solution of Eq. (11) allows one to construct the optical absorption spectrum from the imaginary part of the macroscopic dielectric function ε_M:

$$\mathrm{Im}[\varepsilon_{\mathrm{M}}(\omega)] = 16\pi e^2/\omega^2 \sum_{\mathrm{S}} |\hat{\mathbf{e}}\cdot <0|i/\hbar[H, \mathbf{r}]|\mathrm{S}>|^2 \delta(\omega - \Omega_{\mathrm{S}}) \tag{12}$$

*Vertex corrections and self-consistency tend to cancel to a large extent for the 3D homogeneous electron gas. This cancellation of vertex corrections with self-consistency seems to be a quite general feature. However, there is no formal justification for it and further work along the direction of including consistently dynamical effects and vertex corrections should be explored (Aryasetiawan and Gunnarsson, 1998; and references therein).

where $\hat{\mathbf{e}}$ is the normalized polarization vector of the light and $i/\hbar[H,\mathbf{r}]$ is the single-particle velocity operator. The sum runs over all the excited states $|\mathrm{S}>$ of the system (with excitation energy Ω_S) and $|0>$ is the ground state. One of the main effects of the electron–hole interaction is the coupling of different electron–hole configurations (denoted by $|he>$) which modifies the usual interband transition matrix elements that appear in Eq. (12) to: $<0|i/\hbar[H,\mathbf{r}]|\mathrm{S}> = \sum_h^{\text{holes}} \sum_e^{\text{electrons}} A_\mathrm{S}^{(h,e)} < h|i/\hbar[H,\mathbf{r}]|e>$.

In this context, the Bethe–Salpeter approach to the calculation of two-particle excited states is a natural extension of the GW approach for the calculation of one-particle excited states, within a same theoretical framework and set of approximations (the GW-BSE scheme). As we shall see below, GW-BSE calculations have helped elucidate the optical spectra for a wide range of systems from nanostructures to bulk semiconductors to surfaces and 1D polymers and nanotubes.

5. Applications to Bulk Materials and Surfaces

Since the mid 1980s, the GW approach has been employed with success to the study of quasiparticle excitations in bulk semiconductors and insulators [2, 3, 9, 11, 12]. In Fig. 1, the calculated GW band gaps of a number of insulating materials are plotted against the measured quasiparticle gaps [11]. A perfect agreement between theory and experiment would place the data points on the diagonal line. As seen from the figure, the Kohn–Sham gaps in the local density approximation (LDA) significantly underestimate the experimental values, giving rise to the bandgap problem. Some of the Kohn–Sham gaps are even negative. However, the GW results (which provide an appropriate description of particle-like excitations in an interacting systems) are in excellent agreement with experiments for a range of materials – from the small gap semiconductors such as InSb, to moderate size gap materials such as GaN and solid C_{60}, and to the large gap insulators such as LiF. In addition, the GW quasiparticle band structures for semiconductors and conventional metals in general compare very well with data from photoemission and inverse photoemission measurements.

Figure 2 depicts the calculated quasiparticle band structure of germanium [11] and copper [13] as compared to photoemission data for the occupied states and inverse photoemission data for the unoccupied states. For Ge, the agreement is within the error bars of experiments. In fact, the conduction band energies of Ge were theoretically predicted before the inverse photoemission measurement. The results for Cu agree with photoemission data to within 30 meV for the highest *d*-band, correcting 90% of the LDA error. The energies of the other *d*-bands throughout the Brillouin zone are reproduced within 300 meV, and the maximum error (about 600 meV) is found for the bottom valence band at the Γ

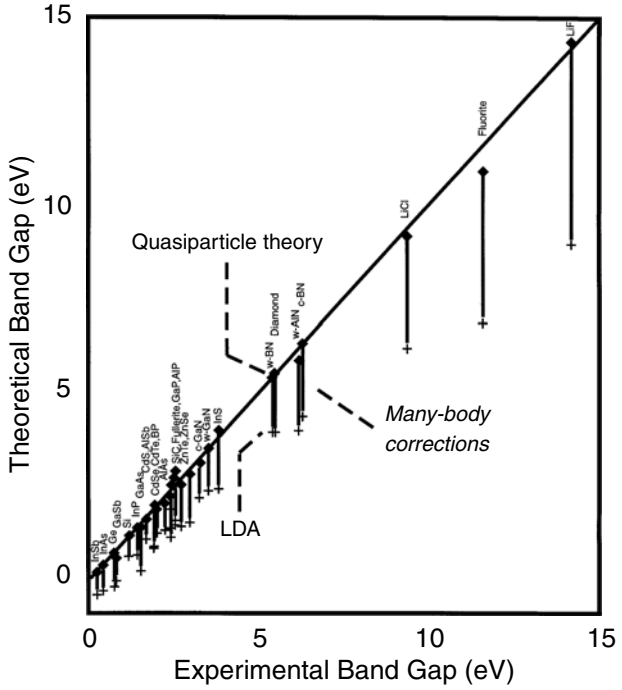

Figure 1. Comparison of the GW bandgap with experiment for a wide range of semiconductors and insulators. The Kohn–Sham eigenvalue gaps calculated within the local density approximation (LDA) are also included for comparison. (after Ref. [11]).

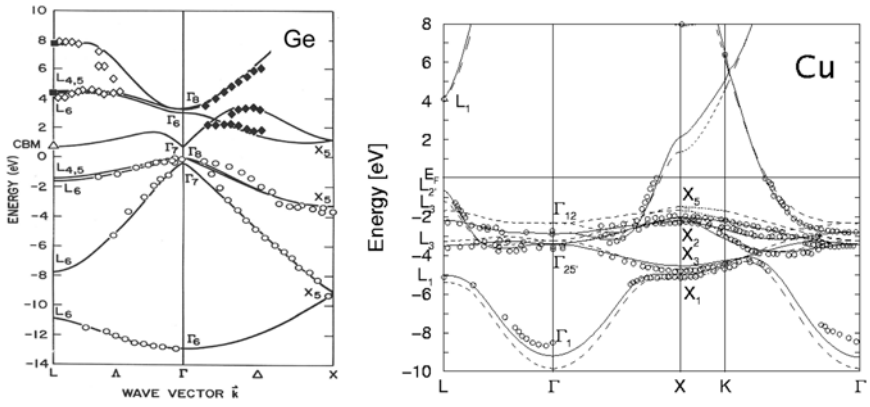

Figure 2. Calculated GW quasiparticle band structure of Ge (left panel) and Cu (right panel) as compared with experiments (open and full symbols). In the case of Cu we also provide the DFT-LDA band structure as dashed lines. (after Ref. [11, 13]).

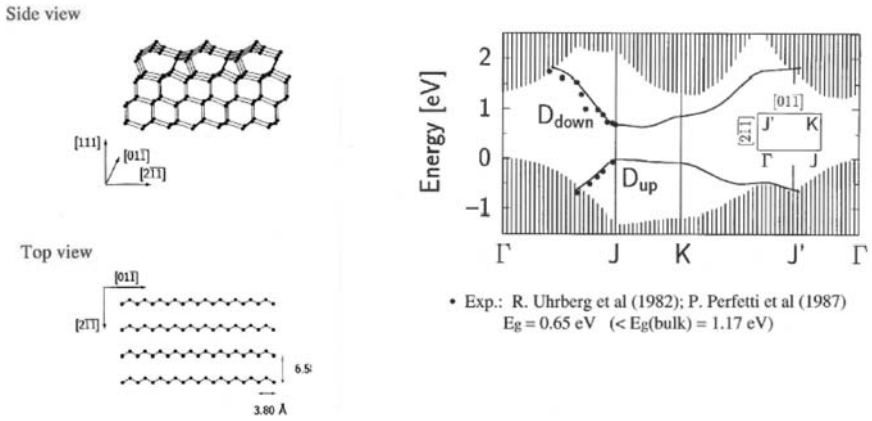

Figure 3. Computed GW quasiparticle bandstructure for the Si(111) 2 × 1 surface compared with experimental results (dots). On the left we show a model of the surface reconstruction (after Ref. [15]).

point, where only 50% of the LDA error is corrected. This level of agreement for the *d*-bands cannot be obtained without including self-energy contributions*. Similar results have been obtained for other materials and even for some non-conventional insulating systems such as the transition metal oxides and metal hydrides.

The GW approach has also been used to investigate the quasiparticle excitation spectrum of surfaces, interfaces and clusters. Figure 3 gives the example of the Si(111)2 × 1 surface [14, 15]. This surface has a very interesting geometric and electronic structure. At low temperature, to minimize the surface energy, the surface undergoes a 2 × 1 reconstruction with the surface atoms forming buckled π-bonded chains. The ensuing structure has an occupied and an unoccupied quasi-1D surface-state band, which are dispersive only along the π-bonded chains and give rise to a quasiparticle surface-state bandgap of 0.7 eV that is very different from the bulk Si bandgap of 1.2 eV. The calculated quasiparticle surface-state bands are compared to photoemission and inversed photoemission data in Fig. 3. As seen in the figure, both the calculated surface-state band dispersion and bandgap are in good agreement with experiment, and these results are also in accord with results from scanning tunneling spectroscopy (STS) which physically also probes quasiparticle excitations. But, a long-standing puzzle in the literature has been that the measured surface-state gap of this system from

*On the other hand, the total bandwidth is still larger than the measured one. This overestimate of the GW bandwidth for metals with respect to the experimental one seems to be a rather general feature, which is not yet properly understood.

optical experiments differs significantly (by nearly 0.3 eV) from the quasiparticle gap, indicative of perhaps very strong electron-hole interaction on this surface. We shall take up this issue later when we discuss optical response.

Owing to interactions with other excitations, quasiparticle excitations in a material are not exact eigenstates of the system and thus possess a finite lifetime. The relaxation lifetimes of excited electrons in solids can be attributed to a variety of inelastic and elastic scattering mechanisms, such as electron–electron (e–e), electron–phonon (e–p), and electron–imperfection interactions. The theoretical framework to investigate the inelastic lifetime of the quasiparticle (due to electron–electron interaction as manifested in the imaginary part of Σ) has been based for many years on the electron gas model of Fermi liquids, characterized by the electron-density parameter r_s. In this simple model for either electrons or holes with energy E very near the Fermi level, the inelastic lifetime is found to be, in the high-density limit ($r_s << 1$), $\tau(E) = 263\, r_s^{-5/2}(E - E_F)^{-2}$ fs, where E and the Fermi energy E_F are expressed in eV [16]. A proper treatment of the electron dynamics (quasiparticle damping rates or lifetimes), however, needs to include bandstructure and dynamical screening effects in order to be in quantitative comparison with experiment. An illustrative example is given in Fig. 4 where the quasiparticle lifetimes of electrons and holes in bulk Cu and Au have been evaluated within the GW scheme, showing an increase in the lifetime close to the Fermi level as compared to the predictions of the free electron gas model. For Au, a major contribution from the occupied d states to the screening yields lifetimes of electrons that are larger than those of electrons in a free-electron-gas model by a factor of about 4.5 for electrons with

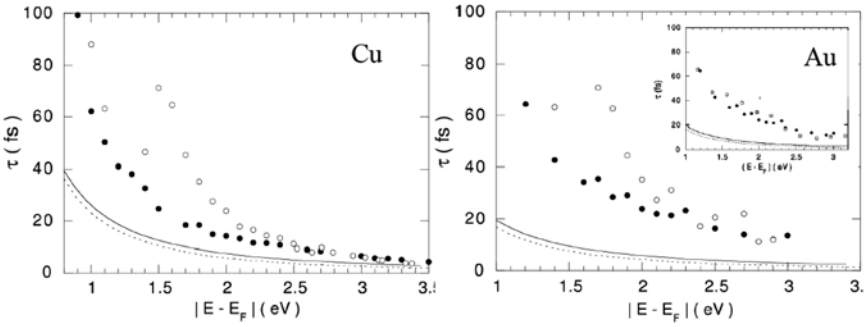

Figure 4. Calculated GW electron and hole lifetimes for Cu and Au. Solid and open circles represent the *ab initio* calculation of $\tau(E)$ for electrons and holes, respectively, as obtained after averaging over wavevectors and the bandstructure for each k vector. The solid and dotted lines represent the corresponding lifetime of electrons (solid line) and holes (dotted line) in a free electron gas with r_s = 2.67 for Cu and r_s = 3.01 for Au. In the inset for Au the theoretical results (solid circles) are compared with experimental data (open circles) from Ref. [17]. (after Refs. [18, 19]).

energies 1–3 eV above the Fermi level. This prediction is in agreement with a recent experimental study of ultrafast electron dynamics in Au(111) films [17].

Up until the late 1990s, the situation for *ab initio* calculation of the optical properties of real materials was, however, not nearly as good as that for the quasiparticle properties. As discussed in Section 4, for the optical response of an interacting electron system, we must also include electron–hole interaction or excitonic effects. The important consequence of such effects is shown in Fig. 5 where the computed absorption spectrum of SiO_2 neglecting electron–hole interaction is compared with the experimental spectrum [20]. There is hardly any resemblance between the spectrum from the non-interacting theory to that of experiment, which has led to extensive debates over the past 40 years on the nature of the four very sharp peaks observed in the experiment. We shall return to this technologically important material later.

With the advance of the GW-BSE method [21–24], accurate *ab initio* calculation of the optical spectra of materials is now possible. As discussed above, solving the Bethe–Salpeter equation yields both the excitation energy and the coupling coefficients among the different electron–hole configurations that form the excited state. The resulting excited-state energies and electron–hole amplitude can then be used to compute the optical (or energy loss and related) spectrum including excitonic effects. The approach has been employed to obtain quite accurately optical transitions to both the bound and continuum states of

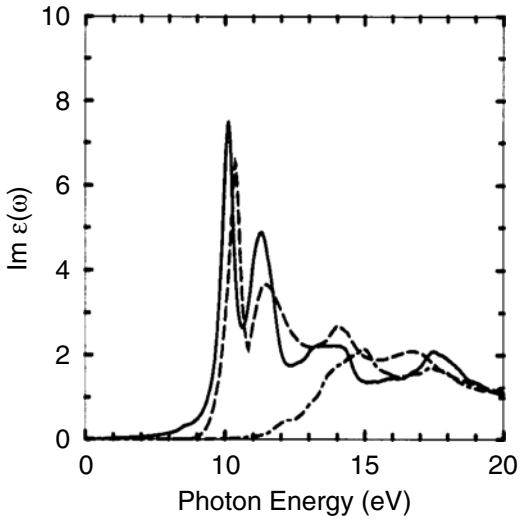

Figure 5. Comparison of the calculated absorption spectrum of SiO_2 including excitonic effects (continuous curve) and neglecting electron–hole interaction (dot-dashed curve) with the experimental spectrum (dashed curve) taken from Ref. [25] (after Ref. [20]).

various materials [7, 10, 21, 22], including reduced dimensional systems and nanostructures.

For bulk GaAs, the GW-BSE results for the optical absorption are compared with experiments in Fig. 6. We see that even for this simple and well-known semiconductor, only with the inclusion of electron–hole interaction then we have good agreement between theory and experiment. The influence of the electron–hole interaction effects extends over an energy range far above the fundamental band gap. As seen from the figure, the optical strength of GaAs is enhanced by nearly a factor of two in the low frequency regime. Also, the electron–hole interaction enhances and shifts the second prominent peak (the so-called E_2 peak) structure at 5 eV to much closer to experiment. This very large shift of about $1/2$ eV in the E_2 peak is not due to a negative shift of the transition energies, as one might naively expect from an attractive electron–hole interaction. The changes in the optical spectrum originate mainly from the coupling of different electron–hole configurations in the excited states, which leads to a constructive coherent superposition of the interband transition oscillator strengths for transitions at lower energies and to a destructive superposition at energies above 5 eV [21, 22].

In addition to the continuum part of the spectrum, one can also get out the bound exciton states near the absorption edge from the Bethe–Salpeter equation from first principles without making use of any effective mass approximation. For the case of GaAs, we see in Table 1 that the theory basically reproduces all the observed bound exciton structures to a very high level of accuracy.

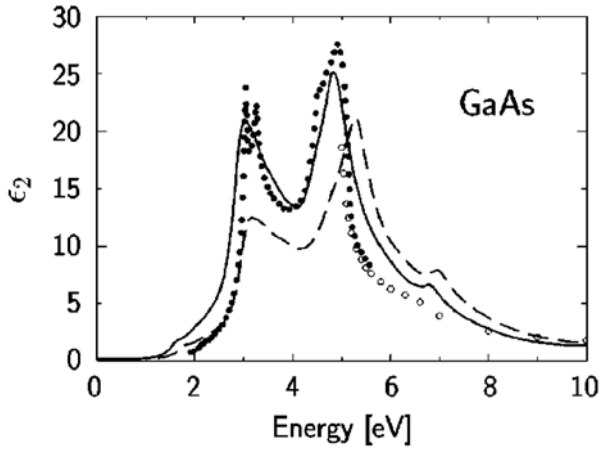

Figure 6. Theoretical (continuous line) and measured (dots) optical absorption spectra for bulk GaAs. The experimental data are taken from Refs. [26, 27]. The calculated spectrum without inclusion of electron–hole interaction (dashed curve) is also given for completeness (after Refs. [21, 22]).

Table 1. Calculated exciton binding energies near the absorption edge for GaAs. The GW-BSE calculations are from [21, 22] and the experimental data are from [26]

Binding energy	Theory (meV)	Experiment (meV)
E_{1s}	4.0	4.2
E_{2s}	0.9	1.0
E_{2p}	0.2–0.7	0–1

The scheme can thus directly be applied to situations in which simple empirical techniques do not hold. Similarly accurate results have been obtained for the other semiconductors.

For larger gap materials, exciton effects are even more dramatic in the optical response as seen for the case of SiO_2 [20] in Fig. 5. The quasiparticle gap of α-quartz is 10 eV. From the *ab initio* calculation, we learn that all the prominent peaks seen in the experiment and also in theory when electron–hole interaction is included are due to transitions to excitonic states. The much-debated peaks in the experimental spectrum are in fact due to the strong correlations between the excited electron and hole in resonant excitonic states since these excited states have energies that are higher than the value for the quasiparticle band gap.

6. Applications to Reduced Dimensional Systems and Nanostructures

The GW-BSE approach in particular has been valuable in explaining and predicting the quasiparticle excitations and optical response of reduced dimensional systems and nanostructures. This is because Coulomb interaction effects in general are more dominant in lower dimensional systems owing to geometrical and symmetry restrictions. As illustrated below, self-energy and electron–hole interaction effects can be orders of magnitude larger in nanostructures than in bulk systems made up of the same elements.

A good example of a reduced dimensional system is the conjugated polymers. The optical properties of these technologically important systems are still far from well understood when compared to conventional semiconductors [28]. For example, there has been much argument in the literature regarding to the binding energy of excitons in polymers such as poly-phenylene-vinylene (PPV); values ranging from 0.1 to 1.0 eV had been suggested. *Ab initio* calculation using the GW-BSE approach show that excitonic effects in PPV are indeed dominant and change qualitative the optical spectrum of the material. This is shown in Fig. 7 where we see that each of the 1D van Hove singularities in the

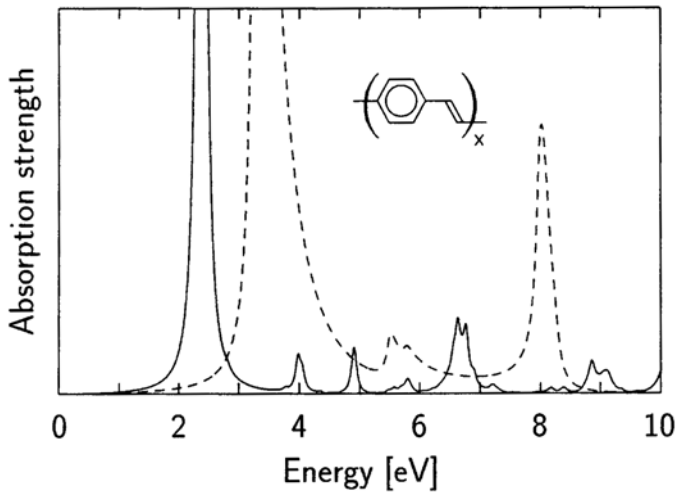

Figure 7. Optical absorption spectra of the polymer PPV. Theoretical results with (continuous line) and without (dashed line) including excitonic effects (after Ref. [28]).

interband absorption spectrum is replaced by a series of sharp peaks due to excitonic states. The lowest optically active exciton is a bound exciton state; but the others are strong resonant exciton states giving rise to peak structures that agree very well with experiment. In particular, when compared to the quasiparticle gap of 3.3 eV, the theoretical results in Fig. 7 yield a very large binding energy of nearly 1 eV for the lowest energy bound exciton in PPV.

The reduced dimensionality at a surface can also greatly enhance excitonic effects. For example, in the case of the Si(111) 2 × 1 surface [28], it is found that the surface optical spectrum at low frequencies is dominated by a surface-state exciton which has a binding energy that is an order of magnitude bigger than that of bulk Si, and one cannot interpret the experimental spectrum without considering the excitonic effects.

This is illustrated in Fig. 8 where the measured differential reflectivity is compared with theory. Here we find that the peak in the differential reflectivity spectrum is dictated by a surface-state exciton with a binding energy of 0.23 eV. This very large binding energy for the surface-state exciton is to be compared to the excitonic binding energy in bulk Si which is only 15 meV. The large enhancement in the electron–hole interaction at this particular surface arises from the quasi-1D nature of the surface states, which are localized along the π-bonded atomic chains on the surface. Similar excitonic calculations for the Ge(111) 2 × 1 reconstructed surface demonstrate how optical differential reflectivity spectra can be used to distinguish between the two possible isomers of the reconstructed surface (see right panel in Fig. 8). This distinction has been enabled by the fact that a quantitative comparison between the calculated

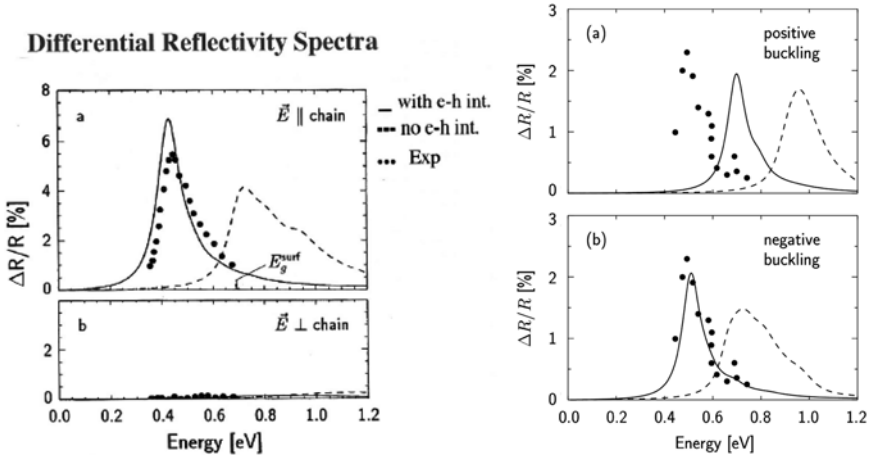

Figure 8. Comparison between experiments and the computed differential reflectivity spectra with and without electron–hole interaction for the Si(111)2 × 1 surface (left panel) [28] and for Ge(111)2 × 1 (right panel) [29].

and experimental spectrum is possible when electron–hole effects are treated correctly [29].

Another 1D system of great current interest is the carbon nanotubes [30]. These are tubular structures of graphene with diameter in the range of one nanometer and length that can be many hundreds of microns or longer. The carbon nanotubes can be metals or semiconductors depending sensitively on their geometric structure, which is indexed by a pair of integers (m, n) where m and n are the two integers specifying the circumferential vector in units of the two primitive translation vectors of graphene. Recent experimental advances have allowed the measurement of the optical response of well-characterized individual, single-walled carbon nanotubes (SWCNTs). For example, absorption measurement on well-aligned samples of SWCNTs of uniform diameter of 4 Å grown inside the channels of zeolites has been performed [31]. And, through the use of photoluminescence excitation techniques, the Rice group has succeeded in measuring both the first and second optical transition energies of well identified, individually isolated, semiconducting SWCNTs [32, 33]. The optical properties of these tubes are found be to quite unusual and cannot be explained by conventional theories. Because of the reduced dimensionality of the nanotubes, many-electron (both quasiparticle and excitonic) effects have been shown to be extraordinarily important in these systems [34, 35].

Figure 9 illustrates the effects of many-electron interactions on the quasiparticle excitation energies of the carbon nanotubes. Plotted in the figure are the quasiparticle corrections to the LDA Kohn–Sham energies for the metallic (3,3) carbon nanotube and the semiconducting (8,0) carbon nanotube.

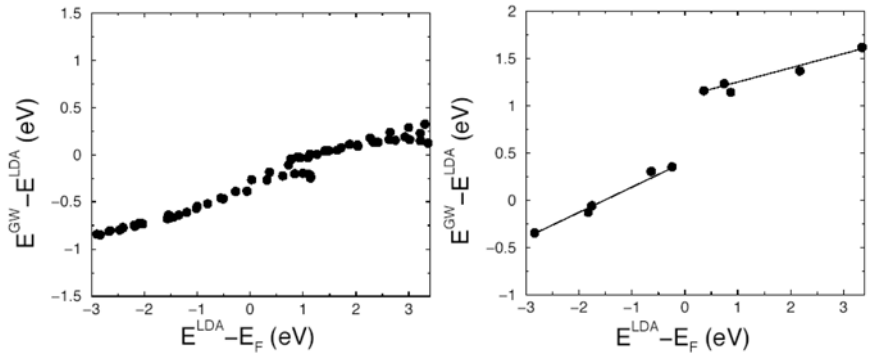

Figure 9. Plot of the quasiparticle corrections to the DFT Kohn–Sham eigenvalues due to self-energy effects as a function of the energy of the states for the metallic (3,3) carbon nanotube (left panel) and the semiconducting (8,0) carbon nanotube (right panel) (after Refs. [34, 35]).

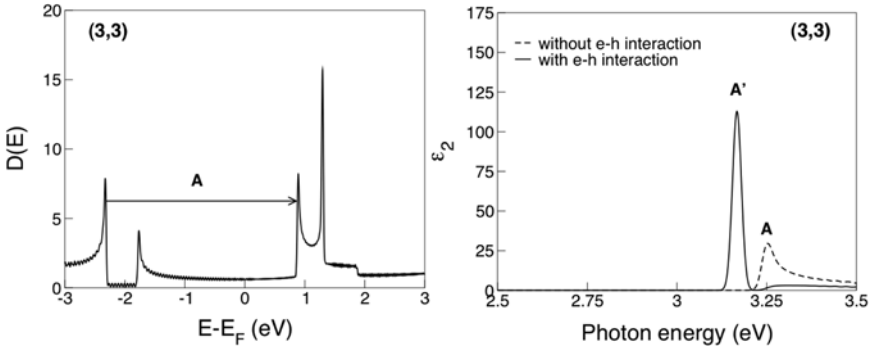

Figure 10. Calculated quasiparticle density of states (left panel) and optical absorption spectrum (right panel) for the (3,3) carbon nanotube (after Refs. [34, 35]).

The general trends are that, for the metallic tubes, the corrections are relatively straight forward. Basically they stretch the bands by ∼15%, as in the case of graphite [11]. But, the self-energy corrections to the quasiparticle energies of the semiconducting tubes are quite large. The corrections cause a large opening of the minimum band gap, as well as a stretching of the bands. As seen in Fig. 9, the self-energy corrections cause the minimum quasiparticle gap of the (8,0) carbon nanotube to open up by nearly 1 eV.

Many-electron interaction effects play an even more important role in the optical response of the carbon nanotubes. The calculated optical spectrum of the metallic (3,3) nanotube (which is one of the 4 Å diameter SWCNTs) is presented in Fig. 10. The left panel shows the electronic density of states. Because of the symmetry of the states, only certain transitions between states (indicated by the arrow A) are optically allowed. The right panel compares the calculated

imaginary part of the dielectric response function between the case with and without electron–hole interactions. The optical spectrum of the (3,3) nanotube is changed qualitatively due to the existence of a bound exciton, even though the system is metallic. This rather surprising result comes from the fact that, although the tube is metallic, there is a symmetric gap in the electron–hole spectrum (i.e., there are no free electron–hole states of the same symmetry as the exciton possible in the energy range of the excitonic state). The symmetry gap is possible here because the (3,3) tube is a 1D metal – i.e., all **k**-states can have well-defined symmetry.

Figure 11 depicts the results for the (5,0) tube, which is another metallic SWCNT of 4 Å in diameter. The surprise here is that, for the range of frequencies considered, the electron–hole interaction in this tube is a net repulsion between the excited electron and hole. Unlike the case of bulk semiconductors, owing to the symmetry of the states involved and metallic screening, the repulsive exchange term dominates over the attractive direct term in the electron–hole interaction. As a consequence, there are no bound exciton states in Fig. 11 and there is a suppression of the optical strength at the van Hove singularities, especially for the second peak in the spectrum.

One expects the above excitonic effects should be even more pronounce in the semiconducting nanotubes. Indeed, this is the case. Figure 12 compares the calculated absorption spectrum of a (8,0) tube between the case with and without electron–hole interactions. The two resulting spectra are qualitatively and dramatically different. When electron–hole interaction effects are included, the spectrum is dominated by bona fide and resonant excitonic states. With interactions, each van Hove singularity structure in the non-interacting spectrum gives rise to a series of exciton states. For the (8,0) tube, the lowest-energy bound exciton has a binding energy of more than 1 eV. Note that the exciton binding energy for bulk semiconductors of similar size bandgap is in general only of the

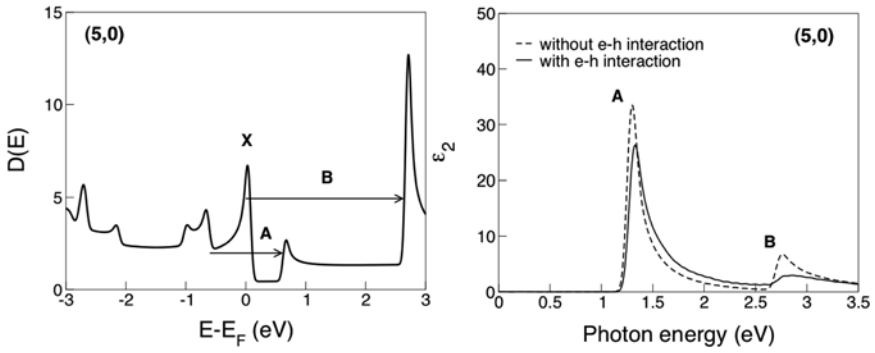

Figure 11. Calculated quasiparticle density of states (left panel) and optical absorption spectrum (right panel) for the (5,0) carbon nanotube (after Refs. [34, 35]).

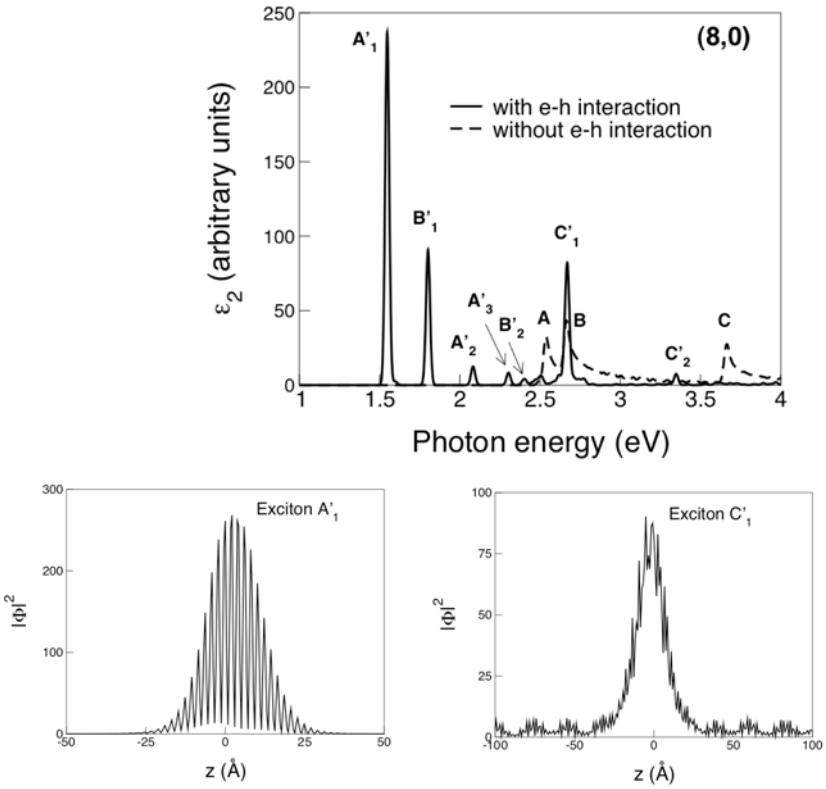

Figure 12. Optical absorption spectra for the (8,0) carbon nanotube (top panel) and the spatial extent of the excitonic wavefunction along the tube axis for a bound and resonant excitonic state (after Refs. [34, 35]).

order of tens of meVs. This illustrates again the dominance of many-electron Coulomb effects in the carbon nanotubes owing to their reduced dimensionality. The bottom two panels in Fig. 12 give the spatial correlation between the excited electron and hole in two of the exciton states, one bound and one resonant state. The extent of the exciton wavefunction is about 25–30 Å for both of these states.

In Table 2 we compare the calculated results for the 4 Å diameter tubes with experimental data. For the samples of 4 Å diameter single-walled carbon nanotubes grown in the channels of the zeolite $AlPO_4$-5 crystal, the Hong Kong group observed three prominent peaks in the optical absorption spectrum [31]. There are only three possible types of carbon nanotubes with a diameter of 4 Å – (5,0), (4,2) and (3,3). All three types of tubes are expected to be present in these samples. The theoretical results quantitatively explain from first principles the three observed peaks and identify their physical origin. The first peak is due to

Table 2. Comparison between experimental [31] and calculated main absorption peaks for all possible 4 Å – (5,0), (4,2) and (3,3) – carbon nanotubes

CNT	Theory (eV)	Experiment (eV)	Character
(5,0)	1.33	1.37	Interband
(4,2)	2.0	2.1	Exciton
(3,3)	3.17	3.1	Exciton

Table 3. Calculated lowest two optical transition energies for the (8,0) and (11,0) carbon nanotubes compared to experimental values [32, 33]. It is noted that the ratio between the two transition energies deviates strongly from the value of 2 predicted by a simple independent-particle model (after Refs. [34, 35])

	(8,0)		(11,0)	
	Experiment	Theory	Experiment	Theory
E_{11}	1.6 eV	1.6 eV	1.2 eV	1.1 eV
E_{22}	1.9 eV	1.8 eV	1.7 eV	1.6 eV
E_{22}/E_{11}	1.19	1.13	1.42	1.45

an interband transition van Hove singularity from the (5,0) tubes, whereas the second peak and third peak are due to the formation of excitons in the (4,2) and (3,3) tubes, respectively [34–36].

The theoretical results [34, 35] on the larger semiconducting tubes have also been used to elucidate the findings from photoluminescence excitation measurements, which yielded detailed information on optical transitions in individual single-walled nanotubes. Table 3 gives a comparison between experiment and theory for the particular cases of the (8,0) and (11,0) tubes. The measured transition energies are in excellent agreement with theory. In particular, we found that the large reduction in the ratio of the second transition energy to the first transition energy E_{22}/E_{11} from the value of 2 (predicted by simple interband transition theory) is due to a combination of factors – bandstructure effects, quasiparticle self-energy effects, and excitonic effects. One must include all these factors to have an understanding of the optical response of the semiconducting carbon nanotubes.

Another example of low-dimensional systems is clusters. In Fig. 13, we show some results on the optical spectra of the Na_4 cluster calculated using the GW-BSE approach as well as those from TDLDA and experiment. The measured spectrum consists of three peaks in the 1.5–3.5 eV range and a broader feature around 4.5 eV. The agreement between results from TDDFT based calculations and GW-BSE calculations is very good. The comparison with the experimental peak positions is also quite good, although the calculated peaks appear shifted to higher energies by approximately 0.2 eV. Good agreement has been obtained for other small semiconductor and metal clusters.

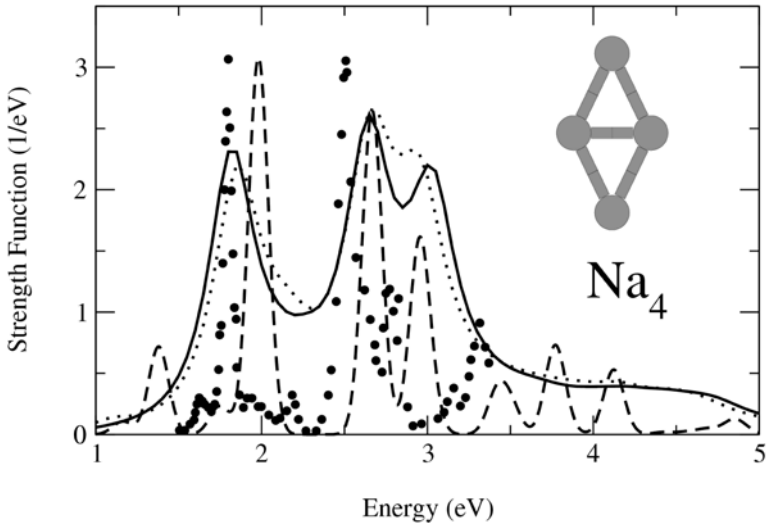

Figure 13. Calculation of the optical absorption (proportional to the strength function) of a Na_4 cluster using the GW-BSE scheme (dashed line) (from Ref. [37]) and with TDDFT using different kernels [38]: TDLDA (solid line), exact-exchange (dotted line). Filled dots represent the experimental results from Ref. [39] (after Ref. [7]).

The above are just several selected examples, given to illustrate the current status in *ab initio* calculations of quasiparticle and optical properties of materials. Similar results have been obtained for the spectroscopic properties of many other moderately correlated electron systems, in particular for semiconducting systems, to a typical level of accuracy of about 0.1 eV.

7. Conclusions and Perspectives

We have discussed in this article the theory and applications of an *ab initio* approach to calculating electron excitation energies, optical spectra, and exciton states in real materials. The approach is based on evaluating the one-particle and the two-particle Green's function, respectively, for the quasiparticle and optical excitations of the interacting electron system, including relevant electron self-energy and electron–hole interaction effects at the GW approximation level. It provides a unified approach to the investigation of both extended and confined systems from first principles. Various applications have shown that the method is capable of describing successfully the spectroscopic properties of a range of systems including semiconductors, insulators, surfaces, conjugated polymers, small clusters, nanotubes and other nanostructures. The agreement between theoretical spectra and data from experiments such as photoemission, tunneling,

optical and related measurements is in general remarkably good for moderately correlated electron systems.

A popular alternative scheme to address optical response is TDDFT. In particular the optical response of simple metal clusters and biomolecules is well reproduced by the standard TDLDA approximation [7, 40]. However, if we increase the size of the system towards a periodic structure in one, two or three dimensions (i.e., polymers, slabs, surfaces or solids), we must be careful with the form of the exchange-correlation functional employed. In contrast to the GW-BSE scheme, difficulties arise when applying TDDFT, for example, to long conjugated molecular chains, where the strong non-locality of the exact functional is not well reproduced in the usual approximations. Similarly, for bulk semiconductors and insulators, the standard functionals fail to describe the optical absorption spectra. The reason has been traced to the fact that the exchange and correlation kernel f_{xc} (which describes the electron–hole interaction within TDDFT) should behave asymptotically, in momentum space, as $1/q^2$ as q goes to 0 [7]. This condition, however, is not satisfied by the LDA or GGA.

Input from the GW-BSE method has in fact been employed to improve the approximate exchange-correlation functionals for use in the TDDFT scheme ([41] and references therein). Such new many-body based f_{xc} has given results on the optical loss spectra of bulk materials such as LiF and SiO_2 that are in quite good agreement with the Bethe–Salpeter equation results and with experiments. (See Fig. 14.) Both spatial nonlocality and frequency dependence of the f_{xc}-kernel turn out to be important in order to properly describe excitonic effects. However, quasiparticle effects still need to be embodied properly within this new approximated TDDFT scheme. An interesting practical question is: which of the two approaches, the GW-BSE method or the TDDFT, would be more efficient in computing the optical properties of the different systems of interest in the future?*

The overall success of the first-principles many-body Green's function approach is impressive and has been highly valued. Nevertheless, the $G_0 W_0$ scheme can be refined in some applications. Studies have shown that: (i) inclusion of vertex corrections improves the description of the absolute position of quasiparticle energies although the amount of such corrections depends sensitively on the model used for the vertex [7, 9]; (ii) vertex effects slightly changes the occupied bandwidth of the homogeneous electron gas, but this correction is not enough to fit the experimental results for metals such as Na; (iii) for the bandwidth of simple metals, self-consistency performed for the homogenous electron gas [42]

*The GW Bethe–Salpeter equation approach offers a clear physical and straightforward picture for the analysis of results and further improvements. It works over a wide range of systems for both quasiparticle and optical excitations. The TDDFT approach, on the other hand, is appealing since it computes optical response more efficiently, but it is appropriate only for neutral excitations and its range of validity is uncertain because of uncontrolled approximations to the functionals.

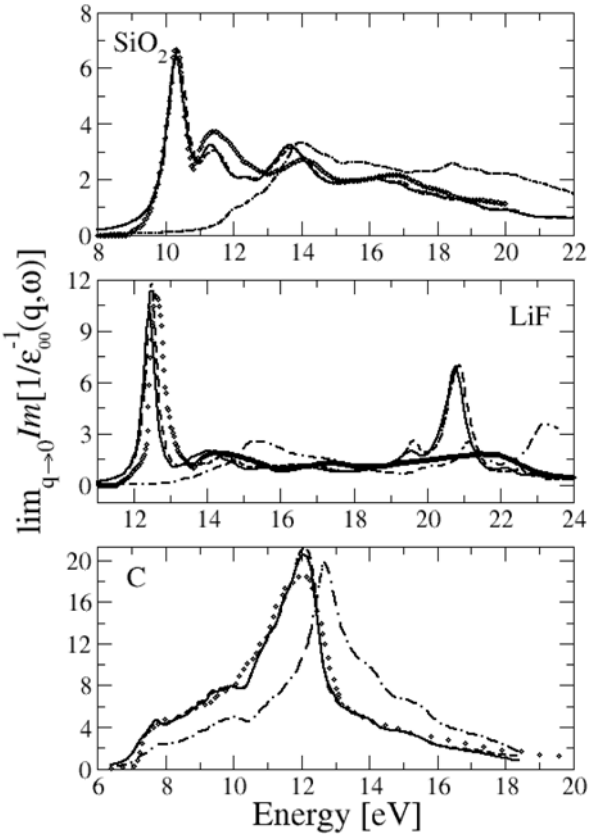

Figure 14. Calculated optical absorption spectra within the GW-BSE approach (continuous line) and those from a new TDDFT f_{xc} kernel derived from the BSE method (dashed line) are compared to experiment (open dots). The independent-quasiparticle response (dashed-dotted line) is also shown (after Ref. [41]).

showed that partially self-consistent GW_0 calculations – in which W is calculated only once using the random-phase-approximation (RPA) so that Eq. (7) is not included in the iterative process – only slightly increase the G_0W_0 occupied bandwidth. Results are even worse at full self-consistency without vertex corrections. The effects of self-consistency thus must be necessarily balanced by the proper inclusion of vertex corrections. This, however, is not the case for the calculation of total energies where the fully self-consistent GW solution appears to provide better results than the partial G_0W_0 procedure. But, if one is interested in spectroscopic properties, a self-consistent GW procedure seems to perform worse than the simpler G_0W_0 scheme.

Experiences from numerous past applications to bulk solids and reduced dimensional systems have demonstrated that in general the GW scheme is an

excellent approximation for the evaluation of the quasiparticle and optical properties of moderately correlated systems. Methods beyond the GW approximation are expected to be required for the study of the spectral features of highly correlated systems. The GW-BSE approach described in this article, however, is arguably the most reliable, practical, and versatile tool we have at present to tackle the optical and electronic response of real material systems from first principles. Further developments in the field should address the proper treatment of self-consistency and vertex corrections. This would further extend the range of applicability of this, already successful, many-body Green's function approach.

References

[1] L. Hedin, "New method for calculating the one-particle Green's function with application to the electron-gas problem," *Phys. Rev.*, 139, A796, 1965.
[2] M.S. Hybertsen and S.G. Louie, "First-principles theory of quasiparticles: calculation of band gaps in semiconductors and insulators," *Phys. Rev. Lett.*, 55, 1418, 1985.
[3] M.S. Hybertsen and S.G. Louie, "Electron correlation in semiconductors and insulators: band gaps and quasiparticle energies," *Phys. Rev. B*, 34, 5390, 1986.
[4] W. Kohn, "Nobel lecture: electronic structure of matter-wave functions and density functionals," *Rev. Mod. Phys.*, 71, 1253, 1999.
[5] E. Runge and E.K.U. Gross, "Density-functional theory for time-dependent systems," *Phys. Rev. Lett.*, 52, 997, 1985.
[6] E.K.U. Gross, J. Dobson, and M. Petersilka, "Density functional theory of time-dependent phenomena," In Density Functional Theory II, R.F. Nalewajski (ed.), *Topics in Current Chemistry*, vol. 181, Springer, Berlin, p. 81, 1986.
[7] G. Onida, L. Reining, and A. Rubio, "Electronic excitations: density functional versus many-body Green's-function approaches," *Rev. Mod. Phys.,* 74, 601, 2002.
[8] L. Hedin and S. Lundqvist, "Effects of electron–electron and electron–phonon interactions on the one electron states of solids," In: H. Ehrenreich, F. Seitz, and D. Turnbull (eds.), S*olid State Physics*, Academic Press, New York, vol. 23, p. 1, 1969.
[9] F. Aryasetiawan and O. Gunnarsson, "GW method," *Rep. Prog. Phys.*, 61, 3, 1998.
[10] M. Rohlfing and S.G. Louie, "Electron–hole excitations and optical spectra from first principles," *Phys. Rev. B*, 62, 4927, 2000.
[11] S.G. Louie, "First-principles theory of electron excitation energies in solids, surfaces, and defects," In: C.Y. Fong (ed.), *Topics in Computational Materials Science*, World Scientific, Singapore, p. 96, 1997.
[12] W.G. Aulbur, L. Jönsson, and J. Wilkins, "Quasiparticle calculations in solids," In: *Solid State Physics*, vol. 54, p. 1, 2000.
[13] A. Marini, G. Onida, and R. Del Sole, "Quasiparticle electronic structure of copper in the GW approximation," *Phys. Rev. Lett.*, 88, 016403, 2002.
[14] J.E. Northrup, M.S. Hybertsen, and S.G. Louie, "Many-body calculation of the surface state energies for Si(111)2 × 1," *Phys. Rev. Lett.*, 66, 500, 1991.
[15] M. Rohlfing and S.G. Louie, "Optical excitations in conjugated polymers," *Phys. Rev. Lett.*, 82, 1959, 1999.
[16] P.M. Echenique, J.M. Pitarke, E. Chulkov, and A. Rubio, "Theory of inelastic lifetimes of low-energy electrons in metals," *Chem. Phys.*, 251, 1, 2000.

[17] J. Cao, Y. Gao, H.E. Elsayed-Ali, R.D.E. Miller, and D.A. Mantell, "Femtosecond photoemission study of ultrafast dynamics in single-crystal Au(111) films," *Phys. Rev. B*, 50, 10948, 1998.
[18] I. Campillo, J.M. Pitarke, A. Rubio, E. Zarate, and P.M. Echenique, "Inelastic lifetimes of hot electrons in real metals," *Phys. Rev. Lett.*, 83, 2230, 1999.
[19] I. Campillo, A. Rubio, J.M. Pitarke, A. Goldman, and P.M. Echenique, "Hole dynamics in noble metals," *Phys. Rev. Lett.*, 85, 3241, 2000.
[20] E.K. Chang, M. Rohlfing, and S.G. Louie, "Excitons and optical properties of alpha-quartz," *Phys. Rev. Lett.*, 85, 2613, 2000.
[21] M. Rohlfing and S.G. Louie, "Excitonic effects and the optical absorption spectrum of hydrogenated Si clusters," *Phys. Rev. Lett.*, 80, 3320, 1998.
[22] M. Rohlfing and S.G. Louie, "Electron–hole excitations in semiconductors and insulators," *Phys. Rev. Lett.*, 81, 2312, 1998.
[23] L.X. Benedict, E.L. Shirley, and R.B. Bohm, "Optical absorption of insulators and the electron–hole interaction: an *ab initio* calculation," *Phys. Rev. Lett.*, 80, 4514, 1998.
[24] S. Albretch, L. Reining, R. Del Sole, and G. Onida, "*Ab initio* calculation of excitonic effects in the optical spectra of semiconductors," *Phys. Rev. Lett.*, 80, 4510, 1998.
[25] H.R. Philipp, "Optical transitions in crystalline and fused quartz," *Solid State Commun.*, 4, 73, 1966.
[26] D.E. Aspnes and A.A. Studna, "Dielectric functions and optical parameters of Si, Ge, GaP, GaAs, GaSb, InP, InAs and InSb frp, 1.5 to 6.0 eV," *Phys. Rev. B*, 27, 985, 1983.
[27] P. Lautenschlager, M. Garriga, S. Logothetisdis, and M. Cardona, "Interband critical points of GaAs and their temperature dependence," *Phys. Rev. B*, 35, 9174, 1987.
[28] M. Rohlfing and S.G. Louie, "Excitations and optical spectrum of the Si(111)-(2 × 1) surface," *Phys. Rev. Lett.*, 83, 856, 1999.
[29] M. Rohlfing, M. Palummo, G. Onida, and R. Del Sole, "Structural and optical properties of the Ge(111)-(2 × 1) surface," *Phys. Rev. Lett.*, 85, 5440, 2000.
[30] S. Iijima, "Helical microtubules of graphitic carbon," *Nature*, 354, 56, 1991.
[31] Z.M. Li, Z.K. Tang, H.J. Liu, N. Wang, C.T. Chan, R. Saito, S. Okada, G.D. Li, J.S. Chen, N. Nagasawa, and S. Tsuda, "Polarized absorption spectra of single-walled 4 Å carbon nanotubes aligned in channels of an $AlPO_4$-5 single crystal," *Phys. Rev. Lett.*, 87, 127401, 2001.
[32] M.J. O'Connell, S.M. Bachilo, C.B. Huffman, V.C. Moore, M.S. Strano, E.H. Haroz, K.L. Rialon, P.J. Boul, W.H. Noon, C. Kittrell, J. Ma, R.H. Hauge, R.B. Weisman, and R.E. Smalley, "Band gap fluorescence from individual single-walled carbon nanotubes," *Science*, 297, 593, 2002.
[33] S.M. Bachilo, M.S. Strano, C. Kittrell, R.H. Hauge, R.E. Smalley, and R.B. Weisman, "Structure-assigned optical spectra of single-walled carbon nanotubes," *Science*, 298, 2361, 2002.
[34] C.D. Spataru, S. Ismail-Beigi, L.X. Benedict, and S.G. Louie, "Excitonic effects and optical spectra of single-walled carbon nanotubes," *Phys. Rev. Lett.*, 92, 077402, 2004.
[35] C.D. Spataru, S. Ismail-Beigi, L.X. Benedict, and S.G. Louie, "Quasiparticle energies, excitonic effects and optical absorption spectra of small-diameter single-walled carbon nanotubes," *Appl. Phys. A*, 78, 1129, 2004.
[36] E. Chang, G. Bussi, A. Ruini, and E. Molinari, "Excitons in carbon nanotubes: an *ab initio* symmetry-based approach," *Phys. Rev. Lett.*, 92, 196401, 2004.
[37] G. Onida, L. Reining, R.W. Godby, and W. Andreoni, "*Ab initio* calculations of the quasiparticle and absorption spectra of clusters: the sodium tetramer," *Phys. Rev. Lett.*, 75, 818, 1995.

[38] M.A.L. Marques, A. Castro, and A. Rubio, "Assesment of exchange-correlation functionals for the calculation of dynamical properties of small clusters in TDDFT," *J. Chem. Phys.*, 115, 3006, 2001. http://www.tddft.org/programs/octopus.

[39] C.R.C. Wang, S. Pollack, D. Cameron, and M.M. Kappes, "Optical absorption spectroscopy of sodium clusters as measured by collinear molecular-beam photodepletion," *J. Chem. Phys.*, 93, 3787, 1990.

[40] M.A.L. Marques, X. López, D. Varsano, A. Castro, and A. Rubio, "Time-dependent density-functional approach for biological photoreceptors: the case of the Green fluorescent protein," *Phys. Rev. Lett.*, 90, 158101, 2003.

[41] A. Marini, R. Del Sole, and A. Rubio, "Bound excitons in time-dependent density-functional-theory: optical and energy-loss spectra," *Phys. Rev. Lett.*, 91, 256402, 2003.

[42] B. Holm and U. von Barth, "Fully self-consistent *GW* self-energy of the electron gas," *Phys. Rev. B*, 57, 2108, 1998.